Enzyme and Microbial Technology 137 (2020) 109515

Contents lists available at ScienceDirect

Enzyme and Microbial Technology

journal homepage: www.elsevier.com/locate/enzmictec

Semi-rational approach to expand the Acyl-CoA Chain length tolerance of *Sphingomonas paucimobilis* serine palmitoyltransferase

Hyunjun Choe, Minsun Cha, Jon D. Stewart*

Department of Chemistry, 126 Sisler Hall, University of Florida, Gainesville, FL 32611 USA

ARTICLE INFO

Keywords:
Serine palmitoyltransferase
C-C bond-forming reaction
Sphingolipids
Enzyme engineering
Enzyme library screening
Substrate tolerance

ABSTRACT

Serine palmitoyltransferase (SPTase), the first enzyme of the sphingolipid biosynthesis pathway, produces 3-ketodihydrosphingosine by a Claisen-like condensation/decarboxylation reaction of L-Ser and palmitoyl-CoA (*n*-C_{16}-CoA). Previous structural analysis of *Sphingomonas paucimobilis* SPTase (*Sp*SPTase) revealed a dynamic active site loop (RPPATP; amino acids 378–383) in which R378 (underlined) forms a salt bridge with the carboxylic acid group of the PLP : L-Ser external aldimine. We hypothesized that this interaction might play a key role in acyl group substrate selectivity and therefore performed site-saturation mutagenesis at position 378 based on semi-rational design to expand tolerance for shorter acyl-CoA's. The resulting library was initially screened for the reaction between L-Ser and dodecanoyl-CoA (*n*-C_{12}-CoA). The most interesting mutant (R378 K) was then purified and compared to wild-type *Sp*SPTase against a panel of acyl-CoA's. These data showed that the R378 K substitution shifted the acyl group preference to shorter chain lengths, opening the possibility of using this and other engineered variants for biocatalytic *C-C* bond-forming reactions.

1. Introduction

Sphingolipids are a class of natural lipids that has drawn significant attention because they control fundamental cellular processes such as regulating cell growth, death, senescence, inflammation, angiogenesis, and intracellular trafficking. Deficiencies in sphingolipid synthesis pathways contribute to several diseases including diabetes, cancer, Alzheimer's disease, and others. [1–3] This has made sphingolipid metabolites, their analogs and the corresponding enzymes important targets for mechanistic studies as well as potential disease treatments. Simple synthetic routes to these compounds as well as their analogs would therefore be highly valuable, prompting us to explore biocatalytic strategies.

Serine palmitoyltransferase (SPTase, EC 2.3.1.50), a member of the α-oxoamine synthase (AOS) family, catalyzes the first step in *de novo* sphingolipid biosynthesis. This pyridoxal 5′-phosphate (PLP)-dependent enzyme performs a Claisen-like condensation/decarboxylation reaction between L-Ser and palmitoyl-CoA (*n*-C_{16}-CoA) to produce the sphingolipid precursor, 3-ketodihydrosphingosine (KDS) (Scheme 1A). Eukaryotic SPTases are heterodimeric, membrane-bound enzymes that have proven difficult to overexpress and characterize. In 2001, however, Ikushiro et al. purified a water-soluble, homodimeric SPTase from *Sphingomonas paucimobilis* EY2395^T (*Sp*SPTase) [4] and successfully overexpressed this enzyme in *E. coli* [5]. Although further study revealed that some bacterial SPTases are also membrane-associated, SPTases from *S. multivorum*, *S. spiritivorum*, and *Bdellovibrio stolpii* were all water-soluble, which significantly improves their ease of study. [6] As *Sp*SPTase shows highest activity out of all characterized bacterial SPTases, we selected *Sp*SPTase for our protein engineering studies.

Apo- and PLP-bound *holo*-forms of *Sp*SPTase were first crystallized by Yard et al., [7] and their structural information has been used to model eukaryotic SPTases [8–11]. *Sp*SPTase and some mutants have been crystallized with ligands to yield the PLP : L-Ser external aldimine intermediate and the PLP : decarboxymyriosin, PLP-inhibitor complex. These structures have contributed greatly to our understanding of the reaction mechanism and the roles of highly conserved residues. [8,12–15]

The currently accepted catalytic mechanism for *Sp*SPTase is shown in Scheme 1B. Catalytic cycles of PLP-dependent enzymes of the AOS family are accompanied by significant conformational changes, enabling the enzymes to control substrate orientation and thereby enhance the rates of individual steps. [16–19] Importantly, acyl-CoA substrate binding often induces conformational changes that increase catalytic activity. For example, formation of the PLP : Gly external aldimine in aminolevulinate synthase is accelerated by at least two orders of magnitude in the presence of succinyl-CoA [20]. Recently, Harrison

* Corresponding author.
E-mail address: jds2@chem.ufl.edu (J.D. Stewart).

https://doi.org/10.1016/j.enzmictec.2020.109515
Received 3 October 2019; Received in revised form 11 January 2020; Accepted 20 January 2020
Available online 21 January 2020
0141-0229/

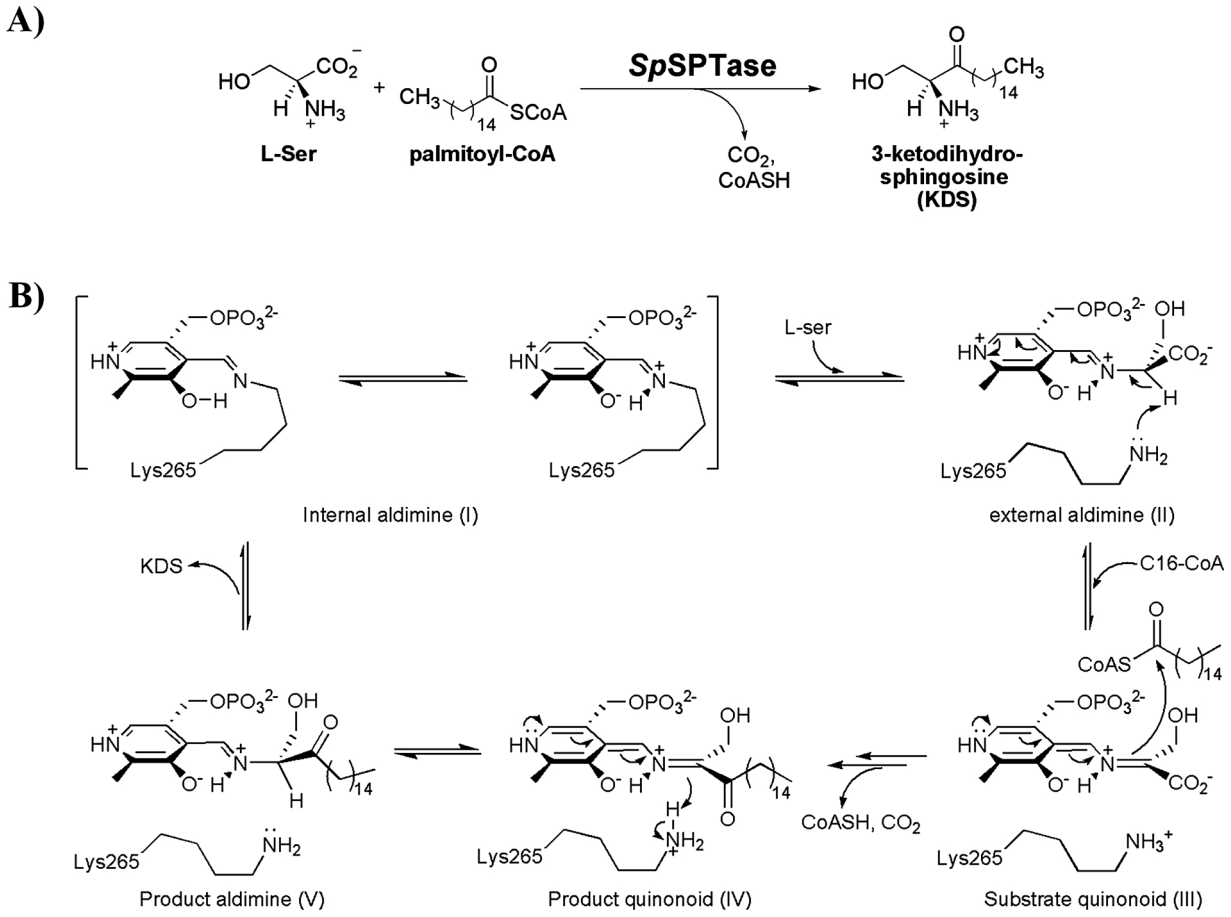

Scheme 1. Reaction and proposed catalytic mechanism of *Sp*SPTase. [21,22,43] A. *Reaction. Sp*SPTase catalyzes the Claisen-like condensation/decarboxylation reaction between L-Ser and palmitoyl (n-C_{16})-CoA. B. *Reaction mechanism.* The Schiff base formed between PLP and the ε-amino group of K265 is in equilibrium between the enolimine and ketoaldimine, forms (internal aldimine, I). External aldimine (II) is formed by transaldimination, and the substrate quinonoid (III) is formed by deprotonation of the L-Ser C_α. The product quinonoid (IV) is formed by acylation and decarboxylation. Reprotonation at the C_α position forms the product aldimine (V). The initial internal aldimine (I) is regenerated by releasing 3-ketodihydrosphingosine (KDS) *via* transaldimination.

and co-workers used L-Ser isotopologues to show that α-carbon deprotonation to form the substrate quinonoid intermediate is rate determining in *Sp*SPTase [21] and that the hydrogen-deuterium exchange rate was increased 100-fold when *S*-(2-oxoheptadecyl)-CoA (a non-hydrolysable analog of n-C_{16}-CoA) was present. [22–24] The coupling between catalysis and acyl-CoA binding makes it challenging to broaden the substrate range of an *Sp*SPTase, and we are unaware of any prior successful reports in this area. It is noteworthy, however, that Ferreira and co-workers were able to alter the substrate preference of a related AOS (aminolevulinate synthase), [25] suggesting that *Sp*SPTase might also be amenable to similar alterations. *Sp*SPTase strongly prefers n-C_{16}-CoA; however, other SPTases sometimes show highest activities with n-C_{14}-CoA or n-C_{18}-CoA. [4,9,26,27] The details that underlie their very slightly different preferences, however, remain unknown.

An active site Arg in *Sp*SPTase (R378), found at the start of a flexible loop that binds the carboxylate of the external aldimine, likewise undergoes large movement during catalytic cycles. [8,28] Raman et al. proposed that R378 plays an important role in stabilizing the enzyme intermediate formed by binding of both L-Ser and n-C_{16}-CoA. This was supported by the observation that the R378A variant was unable to form a quinonoid intermediate in the presence of *S*-(2-oxoheptadecyl)-CoA. [8]

*Sp*SPTase shares high overall sequence similarity (73 %) with other bacterial SPTases and two key active site residues are conserved (H159 and K265), although R378 is not (Fig. 1; Figure S1). The guanidinium group of R378 forms a hydrogen bond with Q357 (also not conserved), which is approximately 15 Å away from the active site in the *apo*-form of the enzyme (Fig. 1A). In the *holo*-form crystal structure, H159 participates in π-π stacking interactions with the pyridinium ring of PLP, and the ε-amino group of K265 forms the Schiff's base with PLP in the internal aldimine (Fig. 1B). In this form, the side chain of R378 remains in the swung-out position. By contrast, this side chain moves to the swung-in position within the active site, forming a salt bridge with the carboxylate group of L-Ser in the PLP : L-Ser external aldimine bound structure (Fig. 1C). In the crystal structure of the K265A *Sp*SPTase mutant with a bound product analog (decarboxymyriosin), the R378 residue reorients to point out of the active site, thereby reestablishing the hydrogen bond with Q357 (Fig. 1D). Raman et al. proved R378 plays a crucial role in the substrate quinonoid intermediate (III) stabilization resulting in a high catalytic activity (Scheme 1B); [8] however, the non-conserved Arg is not essential since R378A and R378 N mutants, in which interaction with the quinonoid intermediate was not possible, had 15- and 35-fold lower catalytic activities, respectively, when tested with the normal substrates.

Here, our goal was to obtain *Sp*STPase variants with even broader substrate tolerance toward shorter acyl-CoA's to enable the synthesis of sphingolipid analogs with shorter and potentially functionalized alkyl chains. Due to the shorter alkyl chain backbones of KDS analogs, sphingolipids derived from the analogs have a higher aqueous solubility, and the modification of the backbone might affect various properties such as cell-permeability and apoptosis-inducing activity. We hypothesized that mutating R378 might affect acyl-CoA substrate specificity as well as catalytic activity since both this residue and the acyl-CoA play important roles in substrate positioning during the catalytic

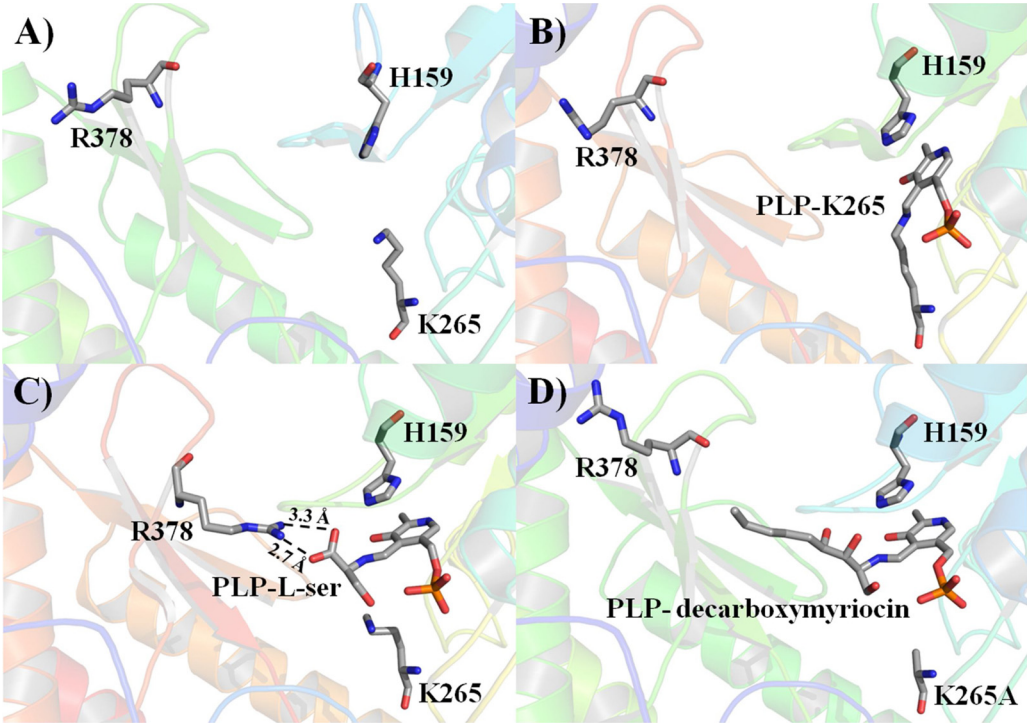

Fig. 1. Structural comparison of *Sp*SPTase in the presence of PLP, PLP : L-Ser, and PLP : decarboxymyriosin. The non-conserved R378 on the mobile loop (RPPATP) as well as highly conserved residues are shown. **A**. *Sp*SPTase without cofactor (PDB 2JGT). [7] **B**. *Sp*SPTase with PLP (PDB 2JG2). [6] **C**. *Sp*SPTase with PLP : L-Ser (PDB 2W8J). [8] **D**. *Sp*SPTase with PLP : decarboxymyriocin (PDB 4BMK,). [15].

cycle. We therefore performed site-saturation mutagenesis at position 378 based on semi-rational design and tested the activities of the variants with L-Ser and several acyl-CoA substrates. These efforts revealed that the R378 K mutant showed higher activities and also preferred shorter alkyl chains acyl-CoA's (particularly n-C_{10} and n-C_{12}) as compared to wild-type *Sp*SPTase.

2. Experimental

2.1. Materials

The *Sp*SPTase gene (GenBank accession: AB055142) with flanking restriction sites was synthesized without codon optimization by GenScript and supplied in a pUC57 vector (although nucleotide ^{336}T was replaced with C to remove the internal *Nde*I restriction site without a codon change). Phusion Hot Start II High-Fidelity DNA Polymerase, restriction enzymes, T4 DNA ligase, and Color Prestained Protein Standard, broad range (11–245 kDa) were purchased from New England Biolabs. Primers were obtained from IDT and Ellman's reagent, L-Ser, and PLP were purchased from ACROS Organics™. Coenzyme A (CoASH) was synthesized from pantethine (purchased from Jarrow Formulas, Inc.) using three *N*-terminally His-tagged *E. coli* enzymes as described previously. [29] Acyl-CoA's were synthesized with anhydrides (purchased from TCI) and purified by adding $MgCl_2$ [30,31]. The synthesis of acyl-CoA's was accelerated by sonication.

2.2. Cloning and site-saturation mutagenesis at position 378

A plasmid containing the complete *Sp*SPTase gene with flanking *Nde*I and *Xho*I restriction sites in pUC57 was transformed into *E. coli* DH5α for amplification. The *Sp*SPTase gene was isolated by digesting with *Nde*I and *Xho*I, ligated between these sites in pET-22b(+) and then the mixture was used to transform *E. coli* DH5α. Plasmid DNA was isolated from randomly-chosen colonies and one with the desired structure (confirmed by Sanger sequencing) was designated plasmid pHC7 and used to transform *E. coli* BL21-Gold (DE3).

For creating a site-saturation library at position 378, mutagenic primers were designed to have high T_m values based on the calculation method previously reported [32] because of the very high GC content (> 74 %) within the primer binding region (T_m = 81.5 + 0.41 (%GC) – (675/N) - % mismatch, where N is the primer length in bases and values for % GC and % mismatch are whole numbers).

The primers used to generate the mutations at position 378 are listed in Table S1. A two-step PCR protocol was performed in a 50 µL total volume containing 5 × Phusion GC Buffer (10 µL), DMSO (10 %), dNTPs (0.2 mM each), forward and reverse primers (0.5 µM each), pHC7 template (2 ng/µL), and DNA polymerase (0.02 U/µL). The reaction was subjected to an initial denaturation step of 98 °C for 30 s followed by 16 cycles of 98 °C for 10 s and 72 °C for 210 s. The final extension was performed at 72 °C (300 s). The reaction product was purified with a Wizard PCR Clean-Up kit (Promega), and then treated with *Dpn*I at 37 °C for 2 h followed by inactivation at 80 °C for 20 min. The amplified DNAs were transformed into *E. coli* BL21-Gold (DE3). Plasmids with the desired mutations were identified by Sanger sequencing.

2.3. Wild-type and mutant SpSPTase activity screening with cell lysates

One microliter aliquots of overnight-cultured mutant cells were transferred to a 96-well plate containing ZYM-5022 autoinduction media 1 mL per well (Table S2), supplemented with ampicillin. The plate was incubated at 30 °C and 350 rpm for 20 h. Cells were harvested by centrifuging 2600 × *g*, then lysed by three cycles of freezing at -80 °C and thawing at 37 °C in 1 mL of lysis buffer (50 mM KP_i, pH 7.5, 150 mM NaCl, and 10 µM PLP). The cell debris was pelleted by centrifugation at 2600 × *g* for 30 min at 4 °C and supernatants were used for SDS-PAGE analysis and an enzyme activity screening with n-C_{12}-CoA. Reactions were carried out on a 96-well plate by adding 10 µL of the cell lysate to 0.2 mL of reaction buffer (500 mM KP_i, pH 7.5, 150 mM NaCl, 20 mM L-Ser, 1 mM EDTA, 10 µM PLP, 0.5 mM n-C_{12}-CoA and 0.3 mM Ellman's reagent). The plate was incubated at 37 °C and A^{412} was monitored for 6 h. Error bars represent standard deviation of duplicate measurement.

2.4. Enzyme activity assays of purified wild-type and R378 K mutant SpSPTases

Wild-type and mutant *Sp*SPTase proteins were overexpressed and purified using Ni-NTA column chromatography as previously reported. [7] All purification steps were performed at 4 °C. Activity assays were performed without removal of imidazole, and UV–vis spectral analysis was performed with *holoenzyme* (PLP-bound form) obtained by dialysis against 20 mM KP_i, pH 7.5, 150 mM NaCl, 10 μM PLP. Enzyme concentrations were determined by the Bradford method [33] using bovine serum albumin as a standard protein and enzyme activity was detected by measuring the free thiol group of CoASH using Ellman's reagent [34]. Enzyme kinetic assays were performed in a reaction buffer (100 mM KP_i, pH 7.5, 150 mM NaCl, 50 mM L-Ser, 10 μM PLP and 0.2 mM Ellman's reagent) at 25 °C. Purified enzymes (final concentration of 1.0–2.6 mM) were used for the activity assays and the A^{412} was monitored. All measurements were carried out at 25 °C. Various concentrations of acyl-CoA substrates were used (75–400 μM *n*-C_{10}-CoA, 50–400 μM *n*-C_{12}-CoA, 20–200 μM *n*-C_{14}-CoA, and 25–200 μM C_{16}-CoA) at a fixed concentration of L-Ser (50 mM). Error bars represent standard deviation of duplicate measurements.

2.5. Spectral characterization of wild-type and mutant SpSPTases

UV-Vis spectra were recorded at room temperature in 20 mM KP_i buffer (pH 7.5) containing 150 mM NaCl, 10 μM PLP and 10 μM enzyme. Changes in A^{425} were plotted against the concentration of L-Ser, then fitted to a hyperbolic saturation curve.

$$\Delta A^{425}{}_{obs} = \frac{\Delta A^{425}{}_{max} \bullet [\text{L-Ser}]}{K_{D,L-Ser} + [\text{L-Ser}]}$$

where ΔA^{425}_{obs} and ΔA^{425}_{max} represent the observed and maximal absorbance change at 425 nm, respectively, [L-Ser] is the concentration of L-serine, and $K_{D,L\text{-}Ser}$ is the dissociation constant for this ligand.

3. Results and discussion

To determine whether the residue at position 378 can impact substrate specificity and catalytic activity, all possible variants at this position were created and screened along with wild-type *Sp*SPTase using L-Ser and *n*-C_{12}-CoA as substrates. SDS-PAGE showed that all proteins were produced at similar levels in ZYM-5022 autoinduction media (Figure S2), so that any changes in catalytic efficiency observed in crude extracts could be ascribed to altered enzyme properties, rather than to differential overexpression levels. Wild-type *Sp*SPTase shows only 18 % relative activity with L-Ser and *n*-C_{12}-CoA as compared to L-Ser and *n*-C_{16}-CoA; [4] our goal was to identify variants with enhanced activity for shorter-chain acyl-CoA's, if possible. After investigating several possible assay methods, we performed the reactions in the presence of Ellman's reagent (5,5′-dithiobis-2-nitrobenzoate, DTNB), which reacts with the free CoASH thiol liberated by the Claisen condensation [35,36]. Cell lysates were used for screening on a 96-well plate (Fig. 2). Although a number of native esterases and thioesterases are also produced in our *E. coli* host, [37] control experiments showed that background hydrolysis of *n*-C_{12}-CoA in crude extracts was negligible, likely because of the high overexpression level of *Sp*SPTase. In the initial screen with *n*-C_{12}-CoA, the A^{412} value for the R378 K variant was *ca.* 3-fold higher than the wild type enzyme; all other variants showed similar or lower activities. To ensure that the proteins were not inactivated by the high concentration of DTNB used (homodimeric *Sp*SPTase has 10 Cys residues, but they are at least 12 Å away from the active site), [38] the A^{412} values were observed over 6 h. The reasonable linearity of these data supports the notion that DTNB inactivation was not a significant problem (Fig. 2, inset). Based on these results, the R378 K variant was selected for further characterization.

Both the wild-type and the R378 K variant were purified by Ni-NTA

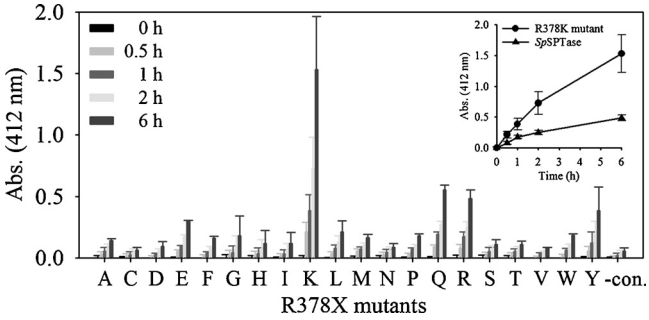

Fig. 2. Activity screening of wild-type *Sp*SPTase and R378X mutants with *n*-C_{12}-CoA.

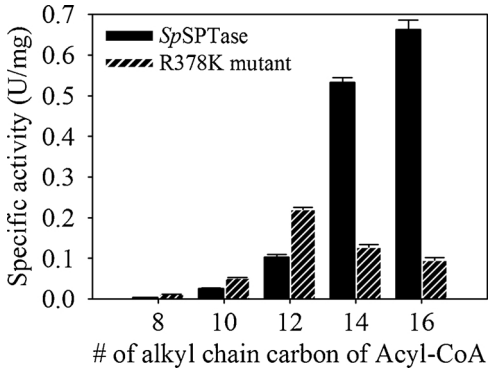

Fig. 3. Specific activities of purified wild-type *Sp*SPTase and the R378 K mutant with various *n*-acyl-CoA's. Reactions were performed by adding the enzymes (final concentration of 50 ng/μL) to a reaction solution containing the specific *n*-acyl-CoA (1.0 mM) along with Ellman's reagent. The reaction was performed at room temperature and the absorbance of DTNB was monitored at 412 nm.

chromatography. The formation of the expected product, 3-keto-C_{14}-dihydrosphingosine, from *n*-C_{12}-CoA and L-Ser by the R378 K mutant was confirmed by MS analysis (Figure S3). A range of acyl-CoA's (*n*-C_8-CoA to *n*-C_{16}-CoA) were also tested with the purified proteins to determine how the R378 K mutation impacted substrate selectivity (Fig. 3). As previously reported, [8] wild-type *Sp*SPTase strongly preferred longer-chain acyl-CoA's (particularly *n*-C_{14}-CoA and *n*-C_{16}-CoA). By contrast, the R378 K mutant showed lower specific activities for *n*-C_{14}-CoA and *n*-C_{16}-CoA but greater efficiencies for *n*-C_{10}- and *n*-C_{12}-CoA's (Fig. 3). These data confirm that the R378 K mutation affects not only catalytic activity but also substrate preference, shifting this to shorter acyl-CoA's. To the best of our knowledge, this is the first example of an engineered SPTase that prefers shorter-chain acyl-CoA's.

The UV–vis spectra of PLP-dependent enzymes serve as useful probes for alterations in the PLP binding site including the enolimine/ketoenamine tautomeric equilibrium as well as intermediate states during catalytic cycle (Fig. 4A). [22,39] The enolimine form of PLP is favored by a nonpolar environment and the complex has an absorption maximum at 330 − 340 nm while the ketoenamine form prefers a more polar environment and the complex shows an absorption maximum at 410 − 430 nm [40]. Altering the polarity of the PLP environment by mutations can change the enolimine and ketoenamine absorbance maxima as well as substrate binding. For example, the N100W and N100Y *Sp*SPTase mutants not only showed shifts in absorbance peaks, but also alterations in the enolimine/ketoenamine tautomeric equilibrium as indicated by a dominant ketoenamine peak at 415 nm as previously described. [8] In contrast to the wild-type *Sp*SPTase, the G385 F mutant showed a noticeable blue shift with maximum absorbance values of 330 nm and 410 nm and 4-fold higher K_d value for L-Ser. [28]

To determine the effects of mutations at position 378 on PLP-

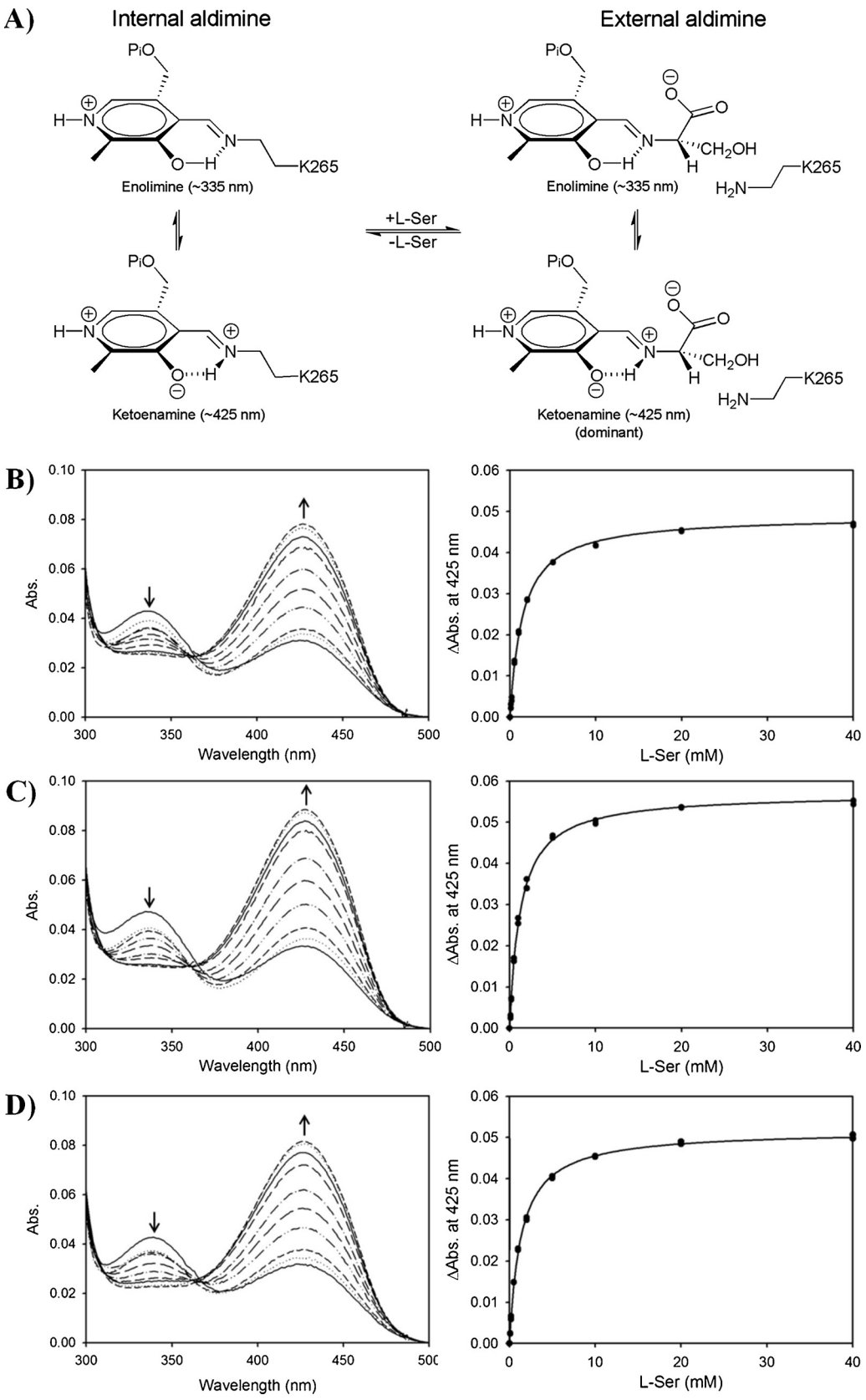

Fig. 4. UV–vis spectral analysis of wild-type *Sp*SPTase and the R378 K and R378A variants. A. Structures of enolimine and ketoenamines. B. Absorbance spectra of wild-type *Sp*SPTase (left) and ΔA^{425} (right) in the presence of varying concentrations of L-Ser. C. Absorbance spectra of R378 K *Sp*SPTase (left) and ΔA^{425} (right) in the presence of varying concentrations of L-Ser. D. Absorbance spectra of R378A *Sp*SPTase (left) and ΔA^{425} (right) in the presence of varying concentrations of L-Ser. For spectra in B – D, the solid line was obtained with *holo*-form enzymes in the absence of L-Ser. The dotted and dashed lines were obtained by increasing the concentration of L-Ser (0.1, 0.2, 0.5, 1, 2, 5, 10, 20, and 40 mM). Spectra were recorded after incubating the enzyme solutions at room temperature for 30 min.

binding, the UV–vis spectra of PLP-bound *holo*-forms were compared for purified wild-type, the R378 K and the R378A *Sp*SPTase variants (Fig. 4B-D, respectively). The spectra were also recorded in the presence of increasing L-Ser concentrations to determine its binding properties. While the maximum absorbance peaks of the R378A *Sp*SPTase were 339 and 423 nm, the corresponding values for both the wild-type and the R378 K *Sp*SPTases were 335 and 425 nm, indicating formation of the internal aldimine (PLP-bound form). The similar

Table 1
Steady-state kinetic parameters for wild-type *Sp*SPTase and the R378 K mutant with various chain length acyl-CoA's.

	Acyl-CoA	k_{cat} (s^{-1})	$K_{M,acyl\text{-}CoA}$ (μM)	$K_{M,L\text{-}Ser}$ (mM)	$k_{cat}/K_{M,acyl\text{-}CoA}$ ($M^{-1}s^{-1}$)	$K_{D,L\text{-}Ser}$ (mM)
wild-type *Sp*SPTase	*n*-C_{10}-CoA	0.034 ± 0.001	680 ± 51		50	1.4 ± 0.1
	n-C_{12}-CoA	0.11 ± 0.01	250 ± 10		440	
	n-C_{14}-CoA	0.76 ± 0.03	80 ± 7		9,500	
	n-C_{16}-CoA	0.85 ± 0.03	41 ± 1	7.2 ± 0.1	21,000	
R378K *Sp*SPTase	*n*-C_{10}-CoA	0.13 ± 0.02	900 ± 150		140	1.2 ± 0.1
	n-C_{12}-CoA	0.35 ± 0.01	560 ± 8		625	
	n-C_{14}-CoA	0.19 ± 0.01	97 ± 6		2,000	
	n-C_{16}-CoA	0.12 ± 0.02	24 ± 1	5.6 ± 0.4	5,000	

spectral profiles for all *holo*-form enzymes showed slightly higher maxima at *ca.* 335 nm as compared to those at 425 nm, suggesting that the PLP local environments were only slightly perturbed by mutations at position 378. The $K_{D,L\text{-}Ser}$ values were calculated from the absorbance changes at 425 nm. The value for wild-type *Sp*SPTase was 1.4 mM, in good agreement with the previously-reported value. [41] The R378 K mutant showed a slightly lower $K_{D,L\text{-}Ser}$ value (1.2 mM), suggesting that the Lys sidechain this location did not significantly stabilize the PLP : L-Ser external aldimine. To investigate the stabilizing effect of the interaction between position 378 and the external aldimine, the external aldimine formation experiment was also performed with R378A mutant (Fig. 4D). Despite lacking a hydrophilic side chain to hydrogen bond with the external aldimine, the R378A mutant showed very similar $K_{D,L\text{-}Ser}$ value (1.34 mM) as wild-type *Sp*SPTase, in a good agreement with the previous report. [8] While position 378 has a large impact on catalytic activity by stabilizing the substrate quinonid intermediate (III), the spectral profiles and $K_{D,L\text{-}Ser}$ values argue that the salt bridge between R378 and the L-Ser carboxylate (Fig. 1C) actually has little stabilizing effect on the external or the internal aldimine.

We measured steady-state kinetic parameters for both wild-type and the R378 K *Sp*SPTases using a series of four acyl-CoA's (*n*-C_{10}-CoA, *n*-C_{12}-CoA, *n*-C_{14}-CoA and *n*-C_{16}-CoA) (Table 1). Values for the wild-type enzyme with *n*-C_{16}-CoA agreed well with previously-reported values.[8,22] Its strong preference for *n*-C_{16}- and *n*-C_{14}-CoA's are due to a combination of lower $K_{M,acyl\text{-}CoA}$ values (41 and 80 μM, respectively) and higher k_{cat} values (0.85 and 0.76 s^{-1}) when compared to shorter-chain acyl-CoA's. By contrast, the R378 K mutant had the highest k_{cat} value for *n*-C_{12}-CoA although that for *n*-C_{10}-CoA was only *ca.* 2.7-fold lower. Its acceptance of shorter-chain acyl-CoA's was largely due to its higher k_{cat} values as compared to the wild-type enzyme. This gave it a broader substrate tolerance, although it preferred shorter-chain acyl-CoA's. Interestingly, the $K_{M,L\text{-}Ser}$ values for both the R378 K mutant and the wild-type enzyme were very similar, showing that the mutation altered acyl-CoA binding almost exclusively.

4. Conclusions

In summary, we have demonstrated that site-saturation mutagenesis based on semi-rational design coupled with screening under auto-induction conditions can be used to impact the substrate range of an SPTase. This opens the possibility of tailoring these *C-C* bond-forming enzymes for new biotechnology applications in chemical synthesis. While other classes of PLP-dependent enzymes have become important tools in chemical synthesis, [42] SPTases have lagged behind. Both UV–vis spectroscopic and kinetic data showed that the R378 K mutation with the flexible active site loop has no effect on PLP binding and external aldimine stabilization, but does significantly impact acyl-CoA specificity as well as catalytic activity. It is hoped that crystallographic studies will reveal the details of how this Lys side-chain controls substrate preference.

CRediT authorship contribution statement

Hyunjun Choe: Methodology, Investigation, Writing - original draft, Writing - review & editing. **Minsun Cha:** . **Jon D. Stewart:** Conceptualization, Supervision, Writing - review & editing.

Declaration of Competing Interest

There are no conflicts to declare.

Acknowledgements

We gratefully acknowledge financial support by the NSF (CHE-1705918) and the U.F. University Scholar Program (M.C.). The Mass Spectrometry Research and Education Center is supported by NIH (S10 OD021758-01A1).

Appendix A. Supplementary data

Supplementary material related to this article can be found, in the online version, at doi:https://doi.org/10.1016/j.enzmictec.2020.109515.

References

[1] T. Kolter, K. Sandhoff, Sphingolipid metabolism diseases, Biochim. Biophys. Acta 1758 (2006) 2057–2079.
[2] F. Bourquin, G. Capitani, M.G. Grütter, PLP-dependent enzymes as entry and exit gates of sphingolipid metabolism, Protein Sci. 20 (2011) 1492–1508.
[3] G. van Echten-Deckert, J. Walter, Sphingolipids: critical players in Alzheimer's disease, Prog. Lipid Res. 51 (2012) 378–393.
[4] H. Ikushiro, H. Hayashi, H. Kagamiyama, A water-soluble homodimeric serine palmitoyltransferase from *Sphingomonas paucimobilis* EY2395^T strain, J. Biol. Chem. 276 (2001) 18249–18256.
[5] H. Ikushiro, H. Hayashi, H. Kagamiyama, Bacterial serine palmitoyltransferase: a water-soluble homodimeric prototype of the eukaryotic enzyme, Biochim. Biophys. Acta 1647 (2003) 116–120.
[6] H. Ikushiro, M.M. Islam, H. Tojo, H. Hayashi, Molecular characterization of membrane-associated soluble serine palmitoyltransferases from *Sphingobacterium multivorum* and *Bdellovibrio stolpii*, J. Bacteriol. 189 (2007) 5749–5761.
[7] B.A. Yard, L.G. Carter, K.A. Johnson, I.M. Overton, M. Dorward, H. Liu, S.A. McMahon, M. Oke, D. Puech, G.J. Barton, J.H. Naismith, D.J. Campopiano, The structure of serine palmitoyltransferase; gateway to sphingolipid biosynthesis, J. Mol. Biol. 370 (2007) 870–886.
[8] M.C.C. Raman, K.A. Johnson, B.A. Yard, J. Lowther, L.G. Carter, J.H. Naismith, D.J. Campopiano, The external aldimine form of serine palmitoyltransferase. Structural, kinetic and spectroscopic analysis of the wild-type enzyme and HSAN1 mutant mimics, J. Biol. Chem. 284 (2009) 17328–17339.
[9] M.C.C. Raman, K.A. Johnson, D.J. Clarke, J.H. Naismith, D.J. Campopiano, The serine palmitoyltransferase from *Sphingomonas wittichii* RW1: an interesting link to an unusual acyl carrier protein, Biopolymers 93 (2010) 811–822.
[10] H. Bode, F. Bourquin, S. Suriyanarayanan, Y. Wei, I. Alecu, A. Othman, A. Von Eckardstein, T. Hornemann, HSAN1 Mutations in serine palmitoyltransferase reveal a close structure-function-phenotype relationship, Hum. Mol. Genet. 25 (2016) 853–865.
[11] J.G. Mina, J.K. Thye, A.Q.I. Alqaisi, L.E. Bird, R.H. Dods, M.K. Grøftehauge, J.A. Mosely, S. Pratt, H. Shams-Eldin, R.T. Schwarz, E. Pohl, P.W. Denny, Functional and phylogenetic evidence of a bacterial origin for the first enzyme in sphingolipid biosynthesis in a phylum of eukaryotic protozoan parasites, J. Biol. Chem. 292 (2017) 12208–12219.
[12] Y. Shiraiwa, H. Ikushiro, H. Hayashi, Multifunctional role of His159 in the catalytic

reaction of serine palmitoyltransferase, J. Biol. Chem. 284 (2009) 15487–15495.
[13] J. Lowther, B.A. Yard, K.A. Johnson, L.G. Carter, V.T. Bhat, M.C. Raman, D.J. Clarke, B. Ramakers, S.A. McMahon, J.H. Naismith, D.J. Campopiano, Inhibition of the PLP-Dependent enzyme serine palmitoyltransferase by cycloserine: evidence for a novel decarboxylative mechanism of inactivation, Mol. Biosyst. 6 (2010) 1682–1693.
[14] H. Ikushiro, H. Hayashi, Mechanistic enzymology of serine palmitoyltransferase, Biochim. Biophys. Acta 1814 (2011) 1474–1480.
[15] J.M. Wadsworth, D.J. Clarke, S.A. McMahon, J.P. Lowther, A.E. Beattie, P.R.R. Landgridge-Smith, H.B. Broughton, T.M. Dunn, J.H. Naismith, D.J. Campopiano, The chemical basis of serine palmitoyltransferase inhibition by myriocin, J. Am. Chem. Soc. 135 (2013) 14276–14285.
[16] H.C. Dunathan, Conformation and Reaction Specificity in Pyridoxal Phosphate Enzymes, Proc. Natl. Acad. Sci. U.S.A. 55 (1966) 712–716.
[17] A.C. Eliot, J.F. Kirsch, Pyridoxal phosphate enzymes: mechanistic, structural, and evolutionary considerations, Ann. Rev. Biochem. 73 (2004) 383–415.
[18] G.A. Hunter, G.C. Ferreira, 5-aminolevulinate synthase: catalysis of the first step of heme biosynthesis, Cell. Mol. Biol. 55 (2009) 102–110.
[19] Y.L. Du, K.S. Ryan, Pyridoxal phosphate-dependent reactions in the biosynthesis of natural products, Nat. Prod. Rep. 36 (2019) 430–457.
[20] G.A. Hunter, G.C. Ferreira, Pre-steady-State reaction of 5-Aminolevulinate synthase, J. Biol. Chem. 274 (1999) 12222–12228.
[21] P.J. Harrison, K. Gable, N. Somashekarappa, V. Kelly, D.J. Clarke, J.H. Naismith, T.M. Dunn, D.J. Campopiano, Use of isotopically labeled substrates reveals kinetic differences between human and bacterial serine palmitoyltransferase, J. Lipid Res. 60 (2019) 953–962.
[22] H. Ikushiro, S. Fujii, Y. Shiraiwa, H. Hayashi, Acceleration of the substrate Cc_{alpha} deprotonation by an analogue of the second substrate Palmitoyl-CoA in serine palmitoyltransferase, J. Biol. Chem. 283 (2008) 7542–7553.
[23] L.A. Paige, G.Q. Zheng, S.A. DeFrees, J.M. Cassady, R.L. Geahlen, *S*-(2-Oxopentadecyl)-CoA, a nonhydrolyzable analogue of myristoyl-CoA, is a potent inhibitor of myristoyl-CoA : protein *N*-myristoyltransferase, J. Med. Chem. 32 (1989) 1665–1667.
[24] D.A. Rudnick, C.A. McWherter, W.J. Rocque, P.J. Lennon, D.P. Getman, J.I. Gordon, Kinetic and structural evidence for a sequential ordered Bi Bi mechanism of catalysis by *Saccharomyces cerevisiae* myristoyl-CoA : protein *N*-myristoyltransferase, J. Biol. Chem. 266 (1991) 9732–9739.
[25] T. Lendrihas, J. Zhang, G.C. Hunter, G.C. Ferreira, Arg-85 and Thr-430 in murine 5-aminolevulinate synthase coordinate acyl-CoA-binding and contribute to substrate specificity, Protein Sci. 18 (2009) 1847–1859.
[26] A.H. Merrill Jr, R.D. Williams, Utilization of different fatty Acyl-CoA thioesters by serine palmitoyltransferase from rat brain, J. Lipid Res. 25 (1984) 185–188.
[27] G. Han, K. Gable, L. Yan, M.J. Allen, W.H. Wilson, P. Moitra, J.M. Harmon, T.M. Dunn, Expression of a novel marine viral single-chain serine palmitoyltransferase and construction of yeast and mammalian single-chain chimera, J. Biol. Chem. 281 (2006) 39935–39942.
[28] A.E. Beattie, S.D. Gupta, L. Frankova, A. Kazlauskaite, J.M. Harmon, T.M. Dunn, D.J. Campopiano, The pyridoxal 5′-phosphate (PLP)-dependent enzyme serine palmitoyltransferase (SPT): effects of the small subunits and insights from bacterial mimics of human hLCB2a HSAN1 mutations, Biomed Res. Int. 194371 (2013) 1–13.
[29] L.M.M. Mouterde, J.D. Stewart, An efficient chemoenzymatic synthesis of coenzyme A and its disulfide, Org. Proc. Res. Develop. 20 (2016) 954–959.
[30] P.V. Vignais, I. Zabin, Synthesis and properties of palmityl adenylate, palmityl coenzyme A, and palmityl glutathione, Biochim. Biophys. Acta 29 (1958) 263–269.
[31] P.P. Constantinides, J.M. Steim, Solubility of palmitoyl-coenzyme A in acyltransferase assay buffers containing magnesium ions, Arch. Biochem. Biophys. 250 (1986) 267–270.
[32] L. Madeira da Silva, L. Vandepas, S.D. Bianco, Mutagenesis and analysis of genetic mutations in the GC-Rich KISS1 receptor sequence identified in humans with reproductive disorders, J. Vis. Exp. 55 (2011) e2897.
[33] M.M. Bradford, A rapid and sensitive method for the quantitation of microgram quantities of protein utilizing the principle of protein-dye binding, Anal. Biochem. 72 (1976) 248–254.
[34] G.L. Ellman, K.D. Courtney, V. Andres Jr., R.M. Featherstone, A new and rapid colorimetric determination of acetylcholinesterase activity, Biochem. Pharmacol. 7 (1961) 88–95.
[35] G.L. Ellman, Tissue sulfhydryl groups, Arch. Biochem. Biophys. 82 (1959) 70–77.
[36] P. Eyer, F. Worek, D. Kiderlen, G. Sinko, A. Stuglin, V. Simeon-Rudolf, E. Reiner, Molar absorption coefficients for the reduced Ellman reagent: reassessment, Anal. Biochem. 312 (2003) 224–227.
[37] E. Kuznetsova, M. Proudfoot, S.A. Sanders, J. Reinking, A. Savchenko, C.H. Arrowsmith, A.M. Edwards, A.F. Yakunin, Enzyme genomics: application of general enzymatic screens to discover new genes, FEMS Microbiol. Rev. 29 (2005) 263–279.
[38] W.X. Tian, R.Y. Hsu, Y.S. Wang, Studies on the reactivity of the essential sulfhydryl groups as conformational probe for the fatty acid synthetase of chicken liver, J. Biol. Chem. 260 (1985) 11375–11387.
[39] J. Lowther, G. Charmier, M.C. Raman, H. Ikushiro, H. Hayashi, D.J. Campopiano, Role of a conserved arginine residue during catalysis in serine palmitoyltransferase, FEBS Lett. 585 (2011) 1729–1734.
[40] S.A. Ahmed, P. McPhie, E.W. Miles, Thermally induced reversible conformational transition of the tryptophan synthase β2 subunit probed by the spectroscopic properties of pyridoxal phosphate and by enzymatic activity, J. Biol. Chem. 271 (1996) 8612–8617.
[41] H. Ikushiro, H. Hayashi, H. Kagamiyama, Reactions of serine palmitoyltransferase with serine and molecular mechanisms of the actions of serine derivatives as inhibitors, Biochemistry 43 (2004) 1082–1092.
[42] J.F. Rocha, A.F. Pina, S.F. Sousa, N.M.F.S.A. Cerqueira, PLP-dependent enzymes as important biocatalysts for the pharmaceutical, chemical and food industries: a structural and mechanistic perspective, Catal. Sci. Technol. (2019), https://doi.org/10.1039/C9CY01210A.
[43] A.E. Beattie, D.J. Clarke, J.M. Wadsworth, J. Lowther, H.L. Sin, D.J. Campopiano, Reconstitution of the pyridoxal 5'-Phosphate (PLP) dependent enzyme serine palmitoyltransferase (SPT) with pyridoxal reveals a crucial role for the phosphate during catalysis, Chem. Commun. (Camb.) 49 (2013) 7058–7060.